

# Periodic Steady State Identification for use in Modelica based AC electrical system simulation

Martin Raphael Kuhn

German Aerospace Center (DLR e.V.), department of system dynamics and control, Germany  
Martin.Kuhn@dlr.de

## Abstract

Analysis of dynamic systems is often carried out at steady state condition. For cyclic systems like rotating machinery, it is not possible to detect this condition by simply monitoring the change rate of their variables, due to their periodicity. This paper focuses on methods for stationary periodic steady state identification of AC electrical systems. An overview of relevant methods is given and mappings of periodic variables to equivalent stationary variables are discussed. Two new periodic steady state monitors based on Short Time Fourier Transformation are proposed. The study was motivated by the need to identify the steady state condition of an aircraft electrical network for power quality checks. An implementation with Modelica tools is demonstrated.

*Keywords:* periodic systems, steady state identification, wavelet, FFT

## 1 Introduction

Testing of power quality criteria of electrical components and networks according to industrial standards, as (MIL-STD-704F,2004), often demands testing in settled condition. When the data is generated from a simulation of the physical system, at best, the system might be initialized in steady-state condition already. For non-linear switching and periodic systems this condition might not be found easily or only approximately from alternative representations, as in (Kuhn et al.,2012). In this case, the time-domain simulation of the system may converge to the exact periodic steady-state condition from a start condition, if the system is internally stable and well damped. The correct estimation of the convergence time becomes crucial if the evaluation of the quality criterion is part of a closed-loop optimization of the system itself. Then the time for simulation to reach steady-state condition, may affect the total time for the optimization process significantly. While the convergence rate may be known analytically for simple systems, generally this is not the case for arbitrary systems. This chapter shows practical methods for testing on the periodic steady-state condition of AC electrical circuits to reduce unnecessary simulation time. Input signals can be simulation results or measurements. It is assumed that the differential algebraic equation system or the loosely coupled subsys-

tem of interest is completely observable via the chosen output.

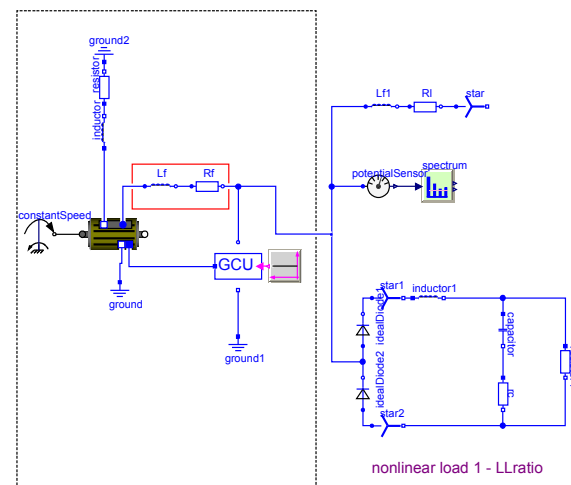


Figure 1: Simulation model for power quality of a small aircraft electrical network

To demonstrate the requirement, we will use the following example of a small aircraft electrical network in Figure 1. It was used as part in a loop of an industrial design process of a generator, whose design parameters are generated by a foregoing routine (Kuhn et al., 2012). The generator feeds a mixed AC resistive and DC 6-pulse switching load. The model simulates through an initial transient phase, till it reaches periodic steady-state. The design is then tested for conformance with industrial standards on power quality in the AC distribution line, which is found between the generator on the left and loads on the right. Power quality is tested via a Fast Fourier Transformation (FFT) Routine block.

The fast identification of periodic steady-state is of wider interest in simulation technique; for example for the non-linear transfer analysis in Saber (Saber,2016) or a similar Modelica-based tool (Bünthe,2011). Both record the input/output behavior of a system, where the input is a frequency sweep signal. Its rate of change is limited in order to arrive -hopefully- in steady-state at the output. The sweep rate may need manual tuning for the specific condition, which may be circumvented by an automatic steady-state detection.

This paper focuses purely on the detection of the periodic steady-state of systems with output  $x(t)$ , which

can be represented by a superposition of band-restricted time-varying harmonic phasors  $X_k(t)$  with base angular velocity  $\omega_{base}$ .

$$x(t) \approx \sum_{k \in K} X_k(t) \cdot e^{jk\omega_{base}t}, K \in \mathbb{Z}, X \in \mathbb{C}, x \in \mathbb{R} \quad (1)$$

The time variant complex variable  $X_k(t)$  is called dynamic phasor

$$X_k(t) = \frac{1}{T} \int_{t-T}^t x(\zeta) e^{-jk\omega_c \zeta} d\zeta \quad (2)$$

The mathematics can be found for example in (Demiray,2008). An example of such a system with time-varying content around distinct frequencies is displayed in Figure 2.

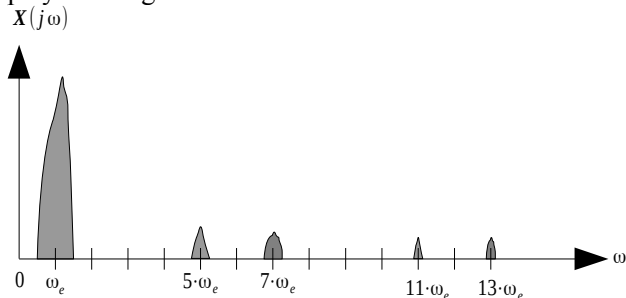


Figure 2: Fourier spectrum of nonstationary signal, with spectral content around  $\sin(\omega_e)$ ,  $\sin(\omega_e \cdot (6 \pm 1))$ ,  $\sin(\omega_e \cdot (12 \pm 1))$

This paper is structured as follows: In the following section the difference between steady-state and periodic steady-state is highlighted. An overview on applicable methods for Steady State Identification is given in section 3. Section 4 discusses the transformation from periodic to non-periodic domain by pre-operators. The main theory of three selected methods for steady-state detection is presented and tested in section 5. This is followed by a conclusion. A theoretical investigation on parametrization of Discrete Fourier Transformation (DFT) for the purpose of Total Harmonic Distortion (THD)-based steady-state detection is given in the Appendix.

## 2 Steady state versus periodic Steady State Identification

In general, a time-variant system  $F(x, \dot{x}, u) = 0$ , excited by input  $u$  or autonomous, may show stable-stationary, unstable-stationary, stable-periodic, unstable-periodic or chaotic behavior of the state variables and possibly of the outputs. For non-linear systems, the system may bifurcate into several possible periodic steady-state conditions (Schupp,2003). For linear differential algebraic systems, a steady-state detection mechanism may search for the condition

$$x(t) - x(t - \Delta t) = 0 \text{ or } \dot{x} = 0 \quad (3)$$

In practical applications only the detection of a minimum convergence rate  $\dot{x} < \alpha_1$  may be feasible, since a longer duration of  $\dot{x} = 0$  may not appear because of asymptotic convergence and/or additive noise. In the case of periodic systems, the steady-state definition has to be adapted. It is called a periodic steady-state condition, where consecutive cycles do not deviate, which means they have an auto-correlation of 1. This can be expressed by

$$x(\tau) - x(\tau - T) = 0 \quad \forall \tau \in [t - T .. t] \quad (4)$$

, where the periodicity time constant  $T$  replaces the infinitesimal  $\Delta t$  in equation 3.

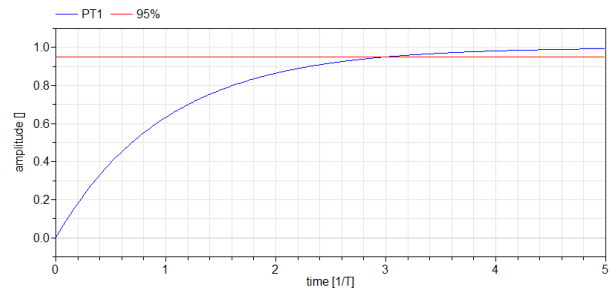


Figure 3: Transient of  $PT_1$  system

To display the difference between steady-state and periodic steady-state, Figure 3 shows the output of a very basic first-order lowpass ( $PT_1$ ) system, excited by a unit step at  $t=0$ . The system is asymptotically internal stable and converges to 1. An amplitude of 0.95 may be seen as quasi steady-state condition, appearing after 3 times characteristic time  $T$ .

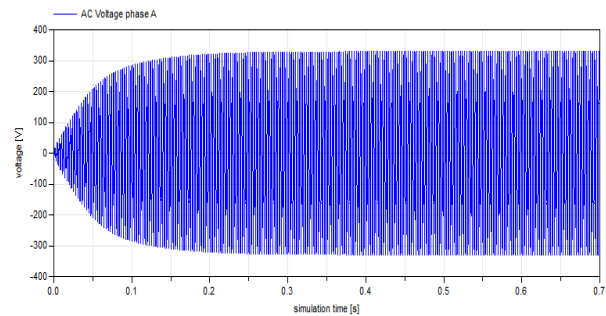


Figure 4: Transient of AC voltage of small aircraft electrical network example (original data)

In contrast to this, the transient of phase A of a three-phase AC voltage of the aircraft electrical network example is plotted in Figure 4. While it is oscillating, at the same time, it shows a first-order like transient behavior of the envelope.

## 3 Overview of methods

The process of signal-based steady-state detection has remarkable analogies with the theory of fault detection. The signal-based fault detection observes the behavior of a system on the change from its nominal (dynamic) behavior. Steady-state detection basically observes the behavior of a system on its change from past behavior.

They differ, as fault detectors generally are designed offline with specific fault data and models; absolute values on nominal or faulty conditions are known. Steady-state observers do not necessarily rely on detailed knowledge of the system. Isermann (Isermann,2006) classifies methods for single signal fault-detection into methods with “limit or trend checking”, and methods with “signal models”. “Limit and trend checking” methods are applicable for measurable absolute values or measures from statistical observers. Detection by “signal models” include correlation methods, spectrum analysis and wavelet analysis. Isermann (Isermann,2006) defines the basic steps of a scheme for fault detection with signal models, as preparation and transformation into “signal model“, extraction of relevant measures by “feature generation” and detection of faults, or by comparison to the nominal behavior in “change detection”.

Similar to it, steady-state detection can be separated into the steps:

- “Signal model” preparation, for periodic systems with removal of oscillation by an operator: The prepared signal can be any property in time domain, frequency domain or stochastic property.
- Application of test on steady-state: The test itself is based on the signal model.
- Decision making: the steady-state decision has to be made. It is very specific to the system, where noise and additional dynamics superpose the potential periodic system and the threshold has to be set based on prior knowledge.

(additive high-frequency noise is not correlated by definition, and should be filtered out from the original signal before, by low pass filtering)

For the steady-state detection, the following methods attracted attention in research in recent years:

The F-like test- developed first by Cao and Rhinehart (Cao and Rhinehart,1995) - belongs to the class of index-based change-detection methods<sup>1</sup>. It relies on statistical methods to identify steady-state in noisy processes. It was tested and expanded on afterwards by Rhinehart for a multi-variable case (Brown and Rhinehart,2000). Applications included different processes, especially in chemical engineering. Other works by Kelly and Hedengren (Kelly and Hedengren,2013) concentrated on slow varying drifts in non-stationary processes with application to a windowed signal.

Wavelet transformation can be used to analyze characteristics of a specific system and match its specific out-

put patterns. Based on this, Jiang (Jiang et al.,2000) developed a method for identification of steps, peaks, noises, abnormal sudden changes and similar for chemical processes and reciprocally steady-state. The technique is not adapted to on-line steady-state detection. However, in an independent work, Korbel (Korbel et al.,2014) developed a steady-state identification for on-line reconciliation, based on wavelet transform and filtering for real-time data.

THD is a quality criterion, which is a measure of the distortion of a base oscillation through its harmonics (multiples). In case where industrial standards demand testing for a specific maximum THD, the criterion needs to be evaluated at periodic steady-state condition. When THD is evaluated repeatedly, observation of convergence of  $\Delta THD$  can be used as a direct indicator of the steady-state condition. This definition is industrially sufficient for the purpose of testing of THD. It was proposed in (Kuhn et al.,2015).

A further method for detecting steady-state is to use auto-regressive exogenous models with exogenous inputs (ARX). This method allows the SSI by system identification, where an auto-regressive model is tuned from the results of simulation or measurements. It is not based on detailed knowledge of the system equations. The identifiability of the system is checked where singularities in the model matrices appear in case of steady-state. Based on this singularity, an index is proposed (Rincón et al.,2015).

From these methods, the “F-like test”, wavelet-based test, THD-based test, and an adaptation of the THD-based test in frequency domain will be discussed in detail in the next sections. The first, due to its popularity and simplicity. The second, as a promising approach and to test the new Modelica Wavelet library. The THD criterion and the adapted frequency-based criterion is chosen, since it relies on the objective criterion directly. An overview is shown in Figure 5.

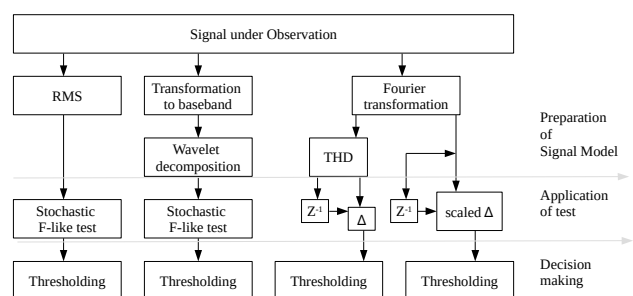


Figure 5: Overview on applied methods

All methods are tested for detection of steady-state on the small electric on-board network example from Figure 1.

<sup>1</sup> A “F-Test“ is a detector of the change in variance

## 4 Mapping of periodic to non-periodic variables

For AC circuits, the method for steady-state testing has to be capable of detecting periodic steady-state. Either by itself, or the signal model preparation has to transform it to an oscillation-free measure. The problem can be overcome by mapping of the periodic signal to a non-cyclic equivalent and identification with standard methods. For a system of type (1), knowledge of a dominating, excited oscillation can be exploited, to identify the steady-state condition of the AC voltage signal. The signals main content is a modulation of a baseband signal  $x_{bb}$  and forced oscillation as

$$x(t) = \Re \{ x_{bb}(t) e^{j\omega_{base} t} \} \quad (5)$$

plus harmonic content at  $k \cdot \omega_{base}$ , plus uncorrelated noise. The minimum periodic cycle is the forced oscillation's time constant  $T_{base} = 2\pi / \omega_{base}$ ,  $2 \cdot T_{base}$  in case of additive odd harmonics, or arbitrary in case of non-harmonic content.

Equation (4) is not useful to implement, since the condition is only fulfilled for perfect congruence. Instead, it can be simplified by using a norm  $\check{x}(t)$ . The steady-state condition can be identified directly via  $\check{x}(t) < \epsilon$  or via some more advanced methods on  $\check{x}(t)$ , listed next.

The test on steady-state can be seen as testing of the auto-regression of the signal, separated in intervals of length  $T$ . And it is similar to regression testing of two signals by the use of norms (e.g. (Pollok and Bender, 2014)). The **maximum error norm** of consecutive periods generates a periodic sampled one-dimensional output:

$$\check{x}_{me}[t] = \max \left( \frac{\|x(\tau) - x(\tau - T)\|}{\|x(\tau)\|} \right) \forall \tau \in [t - T .. t] \quad (6)$$

The norm is quite efficient, due to its simplicity. Since it is a norm on signal amplitude rather than energy, it will penalize sharp discontinuities and noise.

Similar to this and even more easy to implement, by a rough knowledge of the period, only peak values within consecutive periods can be selected. The signal corresponds to sample-and-hold of the peak values with sample period  $T$ . In aeronautical standards, this is often called the **“envelope”**:

$$\check{x}_e[t] = \frac{x(t - \hat{T} .. t) - x(t - 2\hat{T} .. t - T)}{x(t - \hat{T} .. t)} \quad (7)$$

Only one sample is gained within one interval at maximum or in case of application to the absolute value, an additional sample at minimum. Peak values may be prone to noise as some electronics, as rectifiers, add high portions of distortion to the high amplitude part of a voltage wave.

The **temporal** (time limited) **auto-correlation** treats not only minimum and maximum values, but all data of a period. It normalizes the signal to

$$\begin{aligned} \check{x}_{auto}[t] &= \frac{\int_{t-T}^t x(\tau - T) x^*(\tau) d\tau}{\left( \int_{t-2T}^{t-T} |x(\tau)|^2 d\tau \right)^{1/2} \left( \int_{t-T}^t |x(\tau)|^2 d\tau \right)^{1/2}} \\ &= \frac{\int_{t-T}^t x(\tau - T) x^*(\tau) d\tau}{\left( \int_{t-2T}^t |x(\tau)|^2 d\tau \right)^{1/2}} \end{aligned} \quad (8)$$

This norm is tolerant to noise and time shifts but highly prone to incorrect estimation on length of period  $T$ . The temporal auto-correlation measure is similar to the temporal auto-co-variance  $\gamma_{yy}$  of stochastic signals. It is common to think complex or unmodeled processes as stochastic processes (Oppenheim, 1999), which opens the field of stochastic data analysis for the problem. Other coherency metrics on spectrum, energy and time or phase-shift are listed in (Marple and Marino, 2004).

Alternatively the steady-state condition can be seen as the steady-state condition of the baseband signal. When the condition of a cycle is known exactly, it can be identified by one of the following methods:

**AC coupled RMS (Root Mean Square)**: This method is best known for power supply networks at a fixed frequency of 50 or 60 Hz. It can be calculated as by MIL 704f, where RMS is the “value for one half-cycle measured between consecutive zero crossings of the fundamental frequency component”. Information on harmonic contents is lost by the integration.

$$X_{RMS} = \sqrt{\frac{1}{T} \int_0^T x(t)^2 \cdot dt} \quad (9)$$

When the phase angle  $\theta$  is known, mathematical transformations to **phase-fixed reference system** can be applied (e.g. dq0/Park system or Fortescue transformation): For simulation, the phase angle is known. For real electrical systems, for single synchronous generator fed networks, it can be obtained by measuring a machines angular position. Without position measurement, the phase can be derived from the AC voltage by Phase Locked Loops (PLL). A PLL is a control circuit which generates an output signal in proportion to the phase difference of a reference signal to a measured signal. It can be used to adapt the frequency and phase of an observer to the measured signal (Krause et al., 2002).

Alternatively, the base band and harmonics can also be identified by **frequency selective filtering**: Signals can be analyzed in the spectral domain, where the base fre-

quency is usually associated with the spectral content of maximum amplitude. The frequency spectrum can be computed as the correlation of the signal with theoretically infinite sinusoidal waves at certain frequencies (Fourier transformation) or the correlation to finite wave packages at prevailing base frequencies (wavelet transformation (Mallat,2008)). For wavelet transform, one has to distinguish between direct application on sinusoidal signals and application on the pre-processed oscillation-free signal. For finite signals, the Fourier transformation is called Short Time Fourier Transformation, which can be implemented efficiently using Fast Fourier Transformation (FFT) (Cooley and Tukey,1965).

## 5 Implementation and validation of tests

In the following section, the selected theories of Steady State Identification are summarised and the steady-state monitors are tested through experiments.

### 5.1 F-like test

The F-like test, by Cao and Rhinehart (Cao and Rhinehart,1995) is based on statistical measures. The algorithm tests a signal on showing settled distribution at an associated level of significance. Possible distributions are uniform and Gaussian distribution. Measures are variance between data, moving average value and variance in the data itself. This method relies on sampled data.

The following steps can be implemented at low computational effort: First, the sampling vector is filtered by a filter factor of  $\lambda_1$ .

$$X_f[i] = \lambda_1 X[i] + (1 - \lambda_1) \cdot X_f[i-1] \quad (10)$$

Where  $X[i]$  are sampled data,  $X_f[i]$  are filtered values and  $\lambda_1$  is a filter factor. In the second step, a measure of the variance  $v_f^2$  is computed with a moving average filter factor of  $\lambda_2$ :

$$v_f[i]^2 = \lambda_2 (X[i] - X_f[i-1])^2 + (1 - \lambda_2) v_f[i-1]^2 \quad (11)$$

The unbiased estimate of the variance based on the filtered squared deviation from previous filtered values  $var_1$  is given by:

$$var_1[i] = (2 - \lambda_1) \frac{v_f[i]^2}{2} \quad (12)$$

A measure on the second filtered variance estimate  $\delta_f^2$  is calculated based on the filtered square differences of successive data:

$$\delta_f[i]^2 = \lambda_3 (X[i] - X[i-1])^2 + (1 - \lambda_3) \delta_f[i-1]^2 \quad (13)$$

The formula includes a moving average filter with factor  $\lambda_3$ . This second variance  $var_2$  is given by:

$$var_2[i] = \frac{\delta_f[i]^2}{2} \quad (14)$$

Finally, the Steady State Identification index  $R$  is obtained as the ratio of the two variances:

$$R = \frac{(2 - \lambda_1) v_f[i]^2}{\delta_f[i]^2} \quad (15)$$

While  $R$  is a continuous measure, decision making needs tuning of a threshold  $R_t$  to distinguish between steady-state  $R < R_t$  and non steady-state  $R > R_t$ . Filter values have to be tuned to match the time constants of the system under observation. Some more theoretical considerations on correct and incorrect identification of steady-state are given in (Cao and Rhinehart,1995), with respect to different types of error signals.

In a first trial, the F-like test was applied directly on the sinusoidal phase voltage. No useful results could be gained (not plotted), which can be explained by the strong correlation of the sinusoidal shaped signal. Therefore, isolation of the signal of interest had to be conducted first. For this example, simulation results did not show significant difference between several methods of RMS detection. Those are transformation by phase angle, integration over one period with start and end conditions identified by zero crossing detection, and peak-value detection. Figure 7 (top plot) shows the source signal of the test. The AC voltage is mostly settled after 0.1 seconds simulation time with an additional step of 10% at 0.3 seconds.

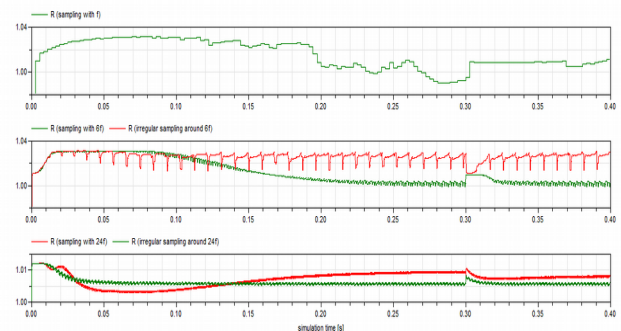


Figure 6: “R” index of F-like test for several sampling rates; input signal see Figure 7, top diagram

The influence of different types of sampling, and therefore different dominating noise on identification index  $R$ , can be seen in Figure 6. The plots present the results of the F-like test, applied on the same source data but with regular sampling intervals 6f and 24f, and irregular sampling around 6f and around 25f. The lambda factors were tuned manually.

It can be clearly seen that the quality of the results diverge on a significant scale. The results based on the 1f

sampling show some slow transient behavior, which is hard to interpret. In contrast, 6f and 24f sampling clearly identify changes. The R statistics show low pass behavior at steps of the input signal. A decision value on steady-state can be set but needs to deal with the chattering around the boundary value  $R_t$ .

### 5.2 Wavelet test

In wavelet analysis, the one-dimensional time variant input signal is decomposed into time variant subspaces with bandpass characteristics. By iterative wavelet multi-level decomposition, the original signal  $f(t)$  is projected into a sequence of nested subspaces; each subspace is characteristic for a spectral content, similar to the indices of the Discrete Fourier Spectrum:

$$f(t) = \sum_{i \in I_j} c_{j,i} \varphi_{j,i} + \sum_{j=1}^J \sum_{k \in k_j} d_{j,k} \psi_{j,k} \quad (16)$$

The first sum represents low frequency content, while the right part represents higher frequency content. The wavelet spectrum originates from iterative bisection of the high-frequency signal up to scale  $J$ .  $\psi_j(t)$  are scaled mother wavelets which define orthogonal spaces. Filtering of a signal corresponds to variation and limiting of its wavelet coefficients  $c_{j,i}$  and  $d_{j,i}$ . Adaptive methods for filtering of Gaussian noise exist in many wavelet toolboxes. The filtered signal in the time domain can be restored by inverse transformation of the conditioned data. Formulas for discrete wavelet transformation are similar.<sup>2</sup>

Similar to the F-like test, this method needs separation of the fundamental of the amplitude-modulated wave first. While this can theoretically be done by an additional wavelet transformation, there is no benefit compared to the RMS method presented before. Next, the signal can be de-noised if necessary. Jiang (Jiang et al.,2003a) proposes to separate the baseband signal into the desired process trend  $T(t)$  and process noise  $N(t)$ , by wavelet multi-level decomposition, filtering and reconstruction. Any other type of continuous or discrete filters may be used equivalently. Although the signal will suffer from a frequency dependent group delay by the filter, for steady-state detection, this can be seen as negligible compared to the typical time scales.

The wavelet-based detection itself uses the fact that a wavelet transform  $Wf(t)$  of a signal  $f(t)$  is proportional to the time derivative of the signal smoothed by the scaling function  $\varphi$  (see wavelet theory for details):

$$Wf(t) = 2 \frac{d}{dt} (f * \varphi)(t) \quad (17)$$

Furthermore, by the wavelet transform of the wavelet transform  $WWf(t)$  one gets an analogon to the second-order derivative. Analogue to assumption of a

steady-state condition as a local extremum where first and second time derivative being zero, single and double wavelet transform can be applied. At a (local) minimum, the conditions

$$Wf(t) < \alpha_{w1}, \quad d(Wf(t))/dt < \alpha_{w2} \quad (18)$$

must hold true. Similarly, for steady-state detection in the time domain, specific scaling of the  $\alpha$  would be necessary. Where an ideal temporal derivative function is unspecific of the frequency and a Fast Fourier Transformation based spectral decomposition lacks information on the temporal variation, a wavelet can be adapted to the “characteristic scale”. This means, the frequency of the wavelet is chosen close to the characteristic response time  $\tau$  of a system which acts as a kind of a bandpass filter. This can be realized by the sampling frequency directly, or iteratively by fragmentation into a wavelet spectrum with narrower bands of equation (16) which is called multi-resolution representation or alternatively Jiang (Jiang et al.,2000) calls it multi-scale process data analysis.

The steady-state index  $\beta(t)$  is calculated from equations (19-21), where  $\theta(t)$  is a factor of combined contributions from the first and second order wavelet and  $\gamma(t)$  is an amplitude-limiting signal operator on the second order wavelet transform.

$$\theta(t) = |Wf(t)| + \gamma(WWf(t)) \quad (19)$$

$$\gamma(WWf(t)) = \begin{cases} 0 & , |WWf| \leq T_w \\ (|WWf| - T_w) / 2 \cdot T_w & , |WWf| \in [T_w, 3 \cdot T_w] \\ 1 & , |WWf| \geq 3 \cdot T_w \end{cases} \quad (20)$$

$\beta$  itself calculates as a threshold comparator from the contributions factor  $\theta(t)$ , with smoothed transient from 0 to 1.

$$\beta(t) = \begin{cases} 0 & , \theta(t) \geq T_u \\ \frac{1}{2} \left[ \cos \left( \frac{\theta(t) - T_s}{T_u - T_s} \cdot \pi \right) + 1 \right] & , T_s < \theta(t) < T_u \\ 1 & , \theta(t) \leq T_s \end{cases} \quad (21)$$

Where  $T_s$  = standard deviation of  $Wf$ ,  $T_u = 3 \cdot T_s$ ,  $T_w$  = median ( $WWf$ ). In  $\beta$ , “zero” indicates unstable status and “one” steady-state condition. For details, see (Jiang et al.,2003b) and for advanced end-of-steady-state-detection see (Korbel et al.,2014).

(Jiang et al.,2003b) demonstrates steady-state detection but does not focus on online implementation. It may look straightforward to perform the analysis continuously on a window of past samples. Practical implementations for this thesis showed the correct choice of the limits  $T_s$ ,  $T_u$  and  $T_w$  often fails when considering only one window. The median especially moves quite arbitrarily. Therefore, limits are calculated non-causally by using the full data set. This proves the con-

<sup>2</sup> For background on wavelet analysis, one may see Debnath (Debnath and Shah,2002), section “Wavelet bases and Multiresolution Analysis”.

siderations of Korbel (Korbel et al.,2014) who proposes to choose the limits from past measurements.

To implement the wavelet test, the Modelica wavelet library (Gao et al.,2014) was used. The library is similar to MATLAB's wavelet toolbox. Since the Modelica wavelet library does not support online computation yet, this study is an offline demonstration only. The library can be developed further for online computation, if issues regarding the initialization of buffers, data storage and allocation of vector sizes of intermediate variables are solved. Furthermore, the plotting relies on Dymola-specific Modelica scripting.

The test makes use of the interpolation routine, definition of a wavelet function and the discrete wavelet transform:

```
Wavelet.General.interpL()
Wavelet.Families.wavFunc(Wavelet.Records.waveletDefinition());
Wavelet.Transform.dwt();
```

Results of the test are displayed in Figure 7: From the original signal, the RMS value is calculated via Park transformation using generator angular information. The RMS value is processed by first and second order wavelet transformation. They show a clear relationship to the temporal derivatives.  $\beta$  is calculated via formulas 19-21. The first steady-state condition is detected at around 0.05 seconds. This assumption is based on the limits  $T_s$ ,  $T_u$  and  $T_w$  and may be changed by different settings.

In summary, the wavelet-based method identifies the steady-state condition of the base harmonic well for the example. The signal can not be processed directly but has to be transformed to a non-periodic representation (RMS). The time scale for the wavelet transform and the limits need to be adapted to the model, based on known prior results. The computational efficiency has to be questioned critically for the wavelet transform. It may be improved in a future, real-time capable implementation of the Modelica library, by use of fast wavelet algorithms.

### 5.3 Discrete Fourier transformation based THD criterion

In (Kuhn et al.,2015) a Total Harmonic Distortion based steady-state detector was proposed. Its "signal model" relies on the Fourier spectrum. According to (Isermann,2006), Fourier spectra are well suited for identification of periodic, stochastic, and non-stationary properties, and therefore for periodic Steady State Identification.

In a first step, a vector of sampled data of the input signal is decomposed into a discrete amplitude-frequency spectrum by a short time Discrete Fourier Transform algorithm. THD is calculated from the spectrum by <sup>3</sup>

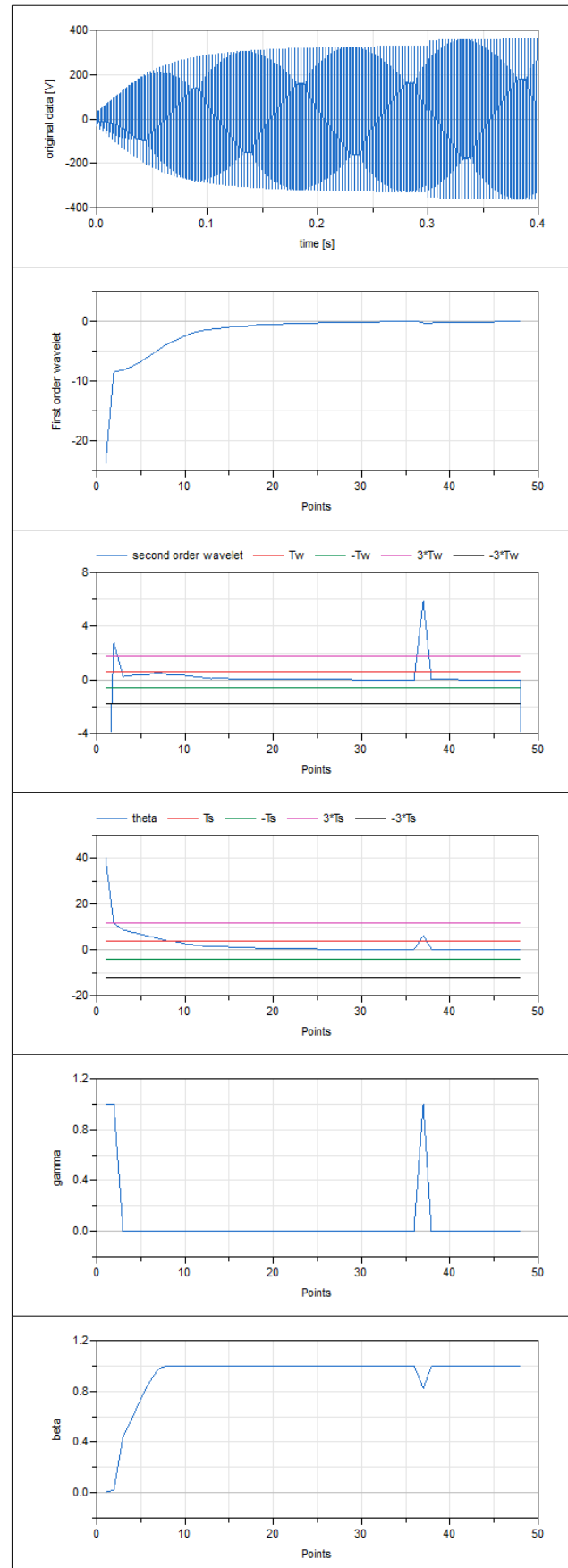


Figure 7: Wavelet based test, results

<sup>3</sup> e.g., IEEE Standard 519-2014 (IEEE,2014)

$$THD = \sqrt{\frac{\sum_{h=2}^M A[h \cdot f_{base}]^2}{A[f_{base}]^2}} \quad (22)$$

It is a one-dimensional norm on the  $M-1$  amplitudes of the harmonics, which is normalized by the amplitude of the base frequency. The phase information and DC component is not considered.

Finally, the steady-state test is designed as a normalized “trend checking”, based on  $\Delta THD$ :

$$y_{THD} = \frac{|THD(t_x) - THD(t_x - N \cdot p)|}{\max(THD, \epsilon)} \quad (23)$$

$y_{THD} < \delta \Rightarrow \text{steady state}$

The criterion relies on consecutive evaluations of the spectra at times  $t_x$  and  $t_x + \Delta T$ . Each evaluation is based on data sets of length  $N[s]$ . The time delay between the two THD windows is defined in proportion  $p$  of the data set length, where an overlap of 50% is proposed for the data sets. Theoretical considerations are derived in section 7.  $\epsilon$  prevents division by zero and influence of noise at small values of  $THD$ . While  $THD$  could be evaluated at every sampling interval, for efficiency reasons, the Modelica algorithm is only evaluated every  $N \cdot p$ . When the frequency resolution is set to  $1/r \cdot f_{base}$ , the total data set length is  $(1+p) \cdot r \cdot T_{base}$  and evaluated no later than  $p \cdot r \cdot T_{base}$  after an event. Example:  $r=4$   $p=1/2 \rightarrow$  criterion evaluation not later than in  $2 \cdot T_{base}$ , based on data set length =  $6 \cdot T_{base}$ .

The main features of the implementation by the Modelica block “WithinAbsoluteFFTDomain\_THD” were already discussed in (Kuhn et al., 2015). It is a big advantage of this method, that the AC signal can be taken directly as an input. There is no need for pre-processing as RMS or transformation to base band. While the expected base frequency should be given roughly, the Modelica-based algorithm can tune itself to the dominating peak in the nearby-spectrum. Also, the block features the option to use the criterion as an indicator for termination of simulation; the THD is delivered as a final result at this steady-state condition. No extra FFT computation is necessary for this, as the computa-

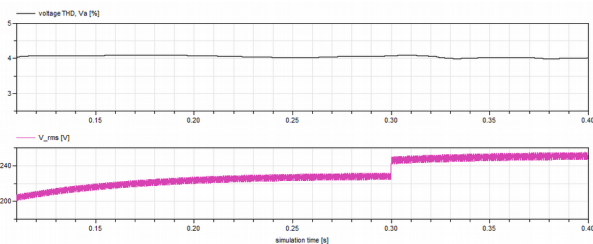


Figure 8: Investigation on spectrum: THD vs. signal (FFT window 0.017s)

tion of THD and THD-based steady-state criterion rely on the same FFT data.

The THD-based criterion was tested with the small grid example. Here, the criterion could NOT identify steady-state condition. This shortcoming can be better understood from the plot of the THD in relation to  $V_{rms}$  in Figure 8, rather than the criterion itself.

As can be seen in the upper plot, the THD is not correlated with the main trend, even at steps. This is a special property of the small grid example. There exist higher harmonics because of the rectifier, but they are in fixed proportion to the base harmonic with fast and well damped filter dynamics on the DC side. Therefore, normalization of THD by the base amplitude prevents a change of the criterion in this case. Furthermore it can be proven easily, it gives the same THD if a  $\Delta$  on one harmonic amplitude compensates for the amplitude on other.

$$THD(t_1) = \sqrt{\frac{A_1^2 + A_2^2 + \dots}{A_b}} \quad (24)$$

$$= THD(t_2) = \sqrt{\frac{(A_1 + \Delta_1)^2 + (A_2 - \Delta_2)^2 + \dots}{A_b}}$$

With proper choice of  $\Delta_1$  and  $\Delta_2$ . Strictly speaking, for the THD identification according to industrial standards, no “real” steady-state condition would be necessary here, as the THD does not change. But since it is not a proper indicator, it is not generally recommended. But it can be adapted to overcome the obstacles as shown next.

Adapted discrete Fourier Transformation-based criterion

In order to overcome the problems of the THD-based steady-state monitor, the new “THD-similar” criterion is proposed:

$$y_{THD\text{similar}} = \max \left( \frac{|A[h \cdot f_{base}[t_x]]|^2 - |A[h \cdot f_{base}[t_x + \Delta T]]|^2}{|A[f_{base}(t_x)]|^2 + \epsilon \cdot |A_{nom}|^2} \right) \quad (25)$$

$\forall h \in [1..M]$ ,

$y_{THD\text{similar}} < \delta \Rightarrow \text{steady state}$

It is also based on the DFT spectrum and is inspired by the THD criterion, maximum error norm and variation in base amplitude. In contrast to THD, also the first (=base) harmonic is considered. An educated guess of a factor  $\epsilon$  of the nominal base amplitude  $A_{nom}$  prevents division by zero and smooths the result. The decision threshold  $\delta$  has to be set based on knowledge from past results.

The criterion and parameterization of FFT is discussed in detail in section 7. It is shown, that this criterion is well suited for identification of steady-state of dynamic

systems (1), where unmodeled dynamics are treated as uniform noise.

The implementation of the function is based on `Within-AbsoluteFFTdomain_THD`, with the same parameters unless stated otherwise. It shares the benefits with the THD approach, with little simulation overhead through the efficient FFT algorithm. As soon as steady-state is detected, the test on conformance with the standards on THD can be performed. The quality test is based on the same FFT data without need for an additional FFT calculation. Results analogue to Figure 6 are shown in Figure 9.

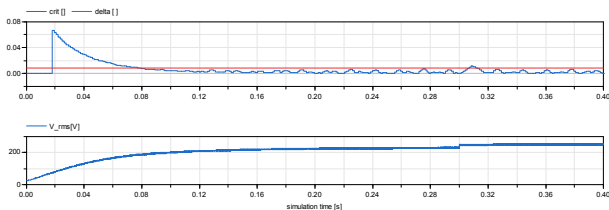


Figure 9: Investigation on new steady-state criterion vs. signal (FFT window 0.017s)

It can be seen that the steady-state condition is found reliably, with proper detection of the initial transient period. The change in amplitude at 0.3 seconds is detected shortly after the event.

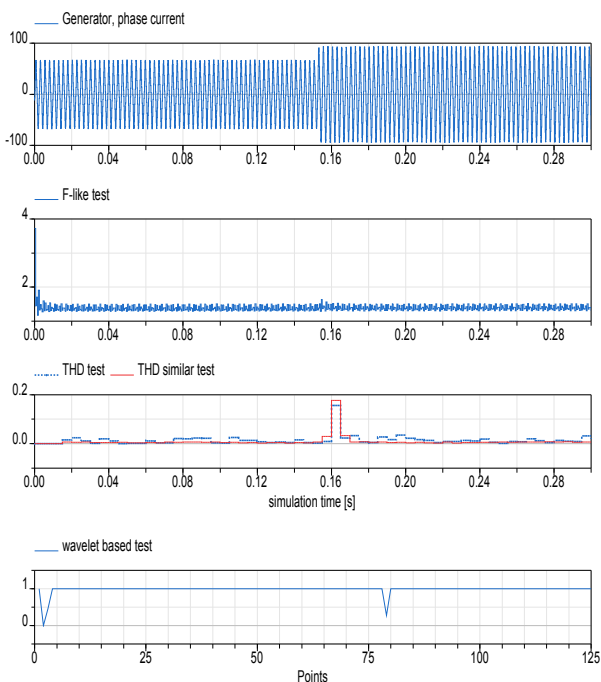


Figure 10: Identification of steady-state, based on real test data

Lastly, all methods are tested with an example based on hardware tests. The top plot in Figure 10 shows the measurement data of a generator connected to an electrical-driven Wing Ice Protection System (WIPS). The load is increased at 0.15seconds. It can be seen that the F-like criterion detects the event, but the output is noisy although care was taken for proper parameteriza-

tion. In contrast to this, the beta parameter of wavelet-based test and THD and THD-similar criterion detect the event reliably, with high signal-to-noise ratio.

## 6 Conclusion

In this paper, procedures for Steady State Identification were tested with an AC electrical circuit, with dominant main amplitude and harmonic distortion, and a second example. Both methods from literature demand a mapping of the periodic to non-periodic signals. The F-like test showed good performance and short delays. However, it was difficult to parameterize, and detection was weak. The wavelet-based test was very successful, but computational overhead and delay is high. Alternatively, an experiment based on a variation of THD was tested. The monitor can treat the periodic signal directly, at medium computational overhead. The delay is high but it can be seen as not critical, since evaluation of THD in steady state is requested. This criterion was not able to detect a transient period, where the signal had a fixed ratio of the base amplitude and harmonics. The THD-similar criterion was designed to also consider the base. Tests were very promising, at medium efficiency and medium delay. Due to its generality and efficiency, this method is proposed as the best choice for the application. The results are summarized in Table 1. Any generalization of the methods demands an investigation with more examples.

Test	Quality of SSI for the examples	Pre-operator needed for AC	Delay	Computation Efficiency
F-like	bad	yes	Short	high
Wavelet based	Very good	yes	high	low
THD criterion	Only partial	no	Medium-high	Medium, low if THD is needed
THD-similar criterion	good	no	Medium-high	Medium, low if THD is needed

Table 1: Evaluation matrix of proposed methods

## Acknowledgements

Some preliminary studies were performed together with Mr. Mohamed Jmari, who did an internship at DLR as part of his studies at ENSMM, Besançon, France.

Valuable input was given by K. Chong.

## 7 Appendix: parametrization of FFT and derived measures for detection of steady-state condition

The following section builds on the results in (Kuhn et al.,2015) and goes into deeper discussion on the parameterization of the Discrete Fourier Transformation needed for THD evaluation, and their influence on steady-state detection. Use of Discrete and Fast Fourier Transformation itself is not discussed here but (Kuhn et

al.,2015) gave a practical approach to the generation of Fourier spectra in Modelica.<sup>4</sup> Computation of FFT might sound numerically demanding, but efficient routines are available as public domain software, or as proprietary software down to chip-optimized routines from Intel and AMD. Cyclic FFT can evaluate the FFT at each sampling step, where results from earlier computations can be reused rather than freshly computed. For practical reasons, one may not evaluate the FFT and THD at every sample, since the convergence of the signal may happen within some AC periods, but not within some sampling intervals.

The FFT algorithm for use by THD calculation is well parameterized by

- The expected base frequency  $f_{base}$  and number of harmonics demanded  $n_{harmonics}$ ; the maximum frequency in the spectrum  $f_{max,FFT}$  needs to be well above the highest treated harmonic:  $f_{max,FFT} > n_{harmonics} \cdot f_{base}$ , where sample frequency  $f_s = 1/T_s = 2 \cdot f_{max,FFT}$
- The type of window function, (e.g. rectangular, Hamming or Butterworth)
- The window length  $N = n_s \cdot T_s = 1/f_{resolution}$ , with the spectral resolution  $f_{resolution}$  and the number of sample points  $n_s$

(proper anti-aliasing by a low-pass filter is assumed).

“Windows” transfer the theoretical unlimited data set to finite length by selection of N samples, where the signal is multiplied by the window function before DFT. Such a window function starts near or at zero, then increases smoothly to a maximum at the center of the time series and decreases again (see Figure 11 for a Hamming window). The theory of DFT implicitly postulates that the input is periodic, where any waveform must repeat itself after the window of sampled signals. This means, for signals with sinusoidal content, the Fourier spectra of temporal consecutive windows coincide: if the windows are of length  $l_p \cdot T_p$ , and time shifted by  $r_p \cdot T_p$ ; with arbitrary integer numbers  $l_p$  and  $r_p$ , and wavelength  $T_p$  for each sinusoidal content  $p$ .

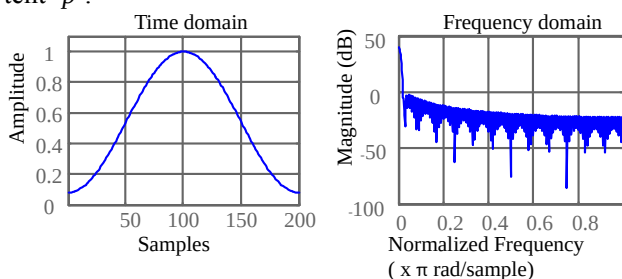


Figure 11: Hamming window

<sup>4</sup> In the meantime the underlying FFT algorithm found its way into the Modelica standard library 3.2.2 as tool independent implementation “Modelica.Math.FastFourierTransform.realFFT()”

In the following, the properties of the spectral analysis are discussed with the purpose of steady-state identification. For better understanding, Figure 12 shows two spectra of the voltage transient of the small aircraft electrical network example: The amplitudes spectrum on the initial transient phase (red) differs from the spectrum of the settled phase (blue) in amplitude and distinctiveness of the peak (a sinusoidal oscillation of infinite length would result in a distinct Dirac impulse). The example shows that the spectra clearly differ and can be used for distinction of steady-state and non steady-state.

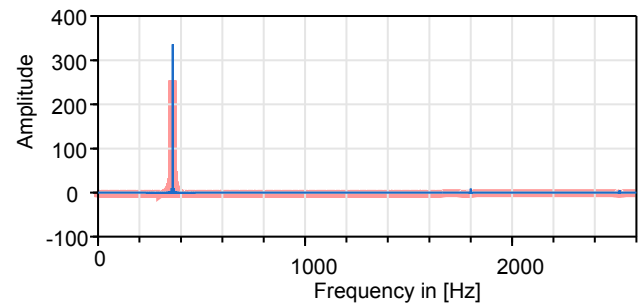


Figure 12: Voltage spectrum of small aircraft electrical network example, with dominant signal  $\sin(2 \cdot \pi \cdot 360 \text{ Hz})$ ; blue: spectrum of period [0..0.2s], red: spectrum of period [0.2..0.4s],

The spectrum can be affected by:

- a) Smearing of peaks, from non-periodicity (energy conservation by Parseval’s theorem) or mismatch of period by window length,
- b) Spectral leakage, from convolution of the spectrum X by the window’s spectrum W
- c) Band restricted variation and smearing of peaks, from unmodeled dynamics

Case a) might be used as an indicator for the variation of the wavelengths, where non-integer  $l_p$  distort the spectrum. This is not recommended. The exact finding of the wavelength or phase information is highly prone to errors. Instead, the discontinuity can be removed by application of a non-rectangular window (Henning etc.)

Case b) can be seen a requirement on the shape and length of the window function. For better understanding, the effect of windowing is demonstrated in Figure 13. It shows the windowing the input signal X (grey peaks) by “rectangular” window (blue) and a “flattop” window (green). The width of the window in frequency domain is indirectly proportional to its length in time domain. The window type itself is characterized by the peak flatness (3dB bandwidth) and peak level of the sidelobes (see overview of window types in (Heinzel et al.,2002)).

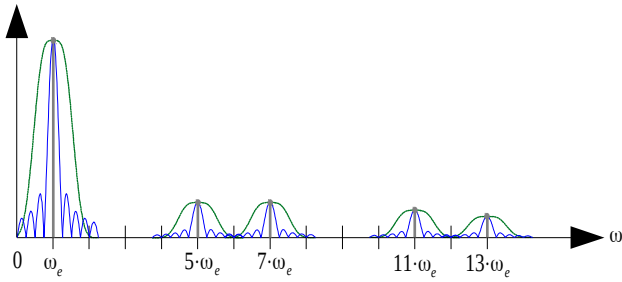


Figure 13: Influence of windowing and sampling

$\mathbf{X}(j\omega)$  (grey): Dirac peaks in continuous Fourier domain, e.g. from sine and cosine

$Y(j\omega)$  (blue): convolution of “rectangular” window with  $\mathbf{X}(j\omega)$

$Y(j\omega)$  (green): convolution of “flattop” window with  $\mathbf{X}(j\omega)$

The convolution of the window with the signal in frequency domain is:

$$Y(e^{j\omega}) = \frac{1}{2\pi} \int_{-\pi}^{\pi} X(e^{j\theta}) W(e^{j(\omega-\theta)}) d\theta \quad (26)$$

The following requirements result, to distinguish tight steady-state and wider non steady-state spectra  $X$  of a signal of type (1):

1) The DFT has to resolve the individual baseband signals of the spectrum, without overlapping caused by the window; (e.g. in Figure 13, the adjacent blue wave packs shall not merge). The window type and length  $n_s \cdot T_s$  have to be chosen with focus on their broadening and height of sidelobes.

2) The steady-state and non-steady-state condition in the basebands of  $X$ , need to have distinguishable amplitudes in discrete  $Y$  as well: The discretization of (26) at a given sampling rate  $f_s$  results in

$$Y[k] = Y(e^{j\omega}) \Big|_{\omega_k = (2\pi/N)k} = \frac{1}{2\pi} \int_{-\pi}^{\pi} X(e^{j\theta}) W(e^{j(\omega_k - \theta)}) d\theta \Big|_{\omega_k = (2\pi/N)k}, \quad (27)$$

$$k = 0..N-1$$

2) is similar to 1), but includes a further demand:  $Y[k]$  may not be undifferentiated for the shapes of  $X$  with the same local area  $c$ :

$$\int_{(2\pi/N)(k-1/2)}^{(2\pi/N)(k+1/2)} X(e^{j\omega}) d\omega = c \quad (28)$$

. This can be the case with flat top windows which makes them not favourable for the purpose of identification of band restricted disturbances: They exhibit broad peaks, with 3dBwidths starting from 2.9 bins. This gives them an approximate characteristics of  $W(e^{j\omega}) = 1$  in the interval around a discretized angular velocity  $\omega_k = (2\pi/N)k \pm 1/2$  (called “bin”). This certainly has benefits for the correct identification of

amplitudes, in case of a frequency mismatch of signal and discretized frequency; but overlapping and visibility of narrow banded effects had to be prevented by high spectral resolution and therefore be paid by large window lengths.

Case c) is by wide the most interesting effect. Steady-state identification can be based on prior knowledge, with measures from a single spectrum. Measures are the amplitudes of the main peaks, or their (3dB) widths, or their amplitude to width ratio, or the ratios of the main peaks. Or it can also be based on the temporal change of these measures. For this work, we assume there is little information on the spectrum given. Furthermore, there is no need to tune the algorithm for a special spectral shape, since any distinct change is seen as non-periodic condition. Instead, a measure is proposed based on the variation of the noise from unmodeled dynamics.

In the 1970s a method called “Welch’s method of averaging modified periodograms” was developed to improve the accuracy of periodograms. Periodograms are estimates of the spectral density of a signal. In this context, “modified” means the window is not of type “rectangular”. According to (Oppenheim and Schaffer, 1998), the estimate  $r$ , of a sequence of  $K$  periodograms is given by

$$I_r(\omega) = \frac{1}{NU} |Y_r(e^{j\omega})|^2 \quad (29)$$

, where estimates are based on non-overlapping data segments of length  $N$ , which are taken from a total data set length  $Q$  by a window. The correction factor  $U$  normalizes the amplitudes of the windows (if not already included in  $Y_r$ ):

$$U = \frac{1}{L} \sum_{n=0}^{N-1} (w[n])^2 \quad (30)$$

Averaging of the  $K$  estimates results in the averaged periodogram

$$\bar{I}(\omega) = \frac{1}{K} \sum_{r=0}^{K-1} I_r(\omega) \quad (31)$$

, respectively

$$\bar{I}[k] = \frac{1}{K} \sum_{r=0}^{K-1} \frac{1}{NU} |Y_r[k]|^2 \quad (32)$$

of a discrete spectrum. In case the properties of the signal remain stationary, and noise is additional and uniformly distributed, the variance of  $\bar{I}(\omega)$  is reduced by a factor of  $1/K$  (Heinzel et al., 2002). Welch (Welch, 1967) proved that other types of windows may be used with similar reduction in variance (modified periodogram). Also he found, that HALF-overlapped windows (see Figure 14) reduce the variation in the spectral components approximately by an additional factor of 2, if this increases the number of windows on the data. More than 50% overlap usually gives no additional benefit, since the cross-correlation of the windows grows. Detailed considerations on the optimal

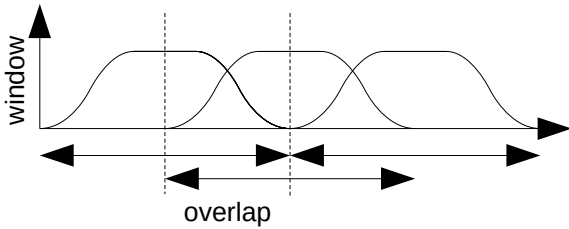


Figure 14: Segmented signal, with three windows and 50% overlap

usage of the information in relation to window overlap, are summarized in (Heinzel et al.,2002). The author lists 33 types of windows with amplitude flatness and power flatness in relation to overlap correlation. Results clearly show, that an overlap of 50% is a good choice for all windows except the “flat top” windows. By Welch’s method it is possible to get better, unbiased estimates of the spectrum, and therefore better inputs for THD calculation. Additionally, with the data of the periodogram (32), the standard deviation of the estimate can be computed with little extra effort. It is possible to construct an F-like test upon these measures, where transition to steady state can be associated with decreasing noise, and therefore decreasing standard deviation. This is not recommended since the large data vector would effect a substantial delay in the steady state detection. Instead, an indicator named ‘randomness’ (Heinzel et al.,2002). is more applicable. It is the ratio of the standard deviation to the averaged estimate of the signal, that dominates the frequency bin under consideration. “Randomness” is near unity for stochastic signals such as noise, and small for coherent signals such as sinusoidal wave:

$$‘randomness’ = \frac{\sigma(\bar{I}[k])}{E(\bar{I}[k])} \quad (33)$$

This “randomness” criterion is proposed as base of the THD-similar steady-state detector. Since reduction of delay is of highest interest, the set of input data must be kept short. This directly results in a number of 2 windows, with an overlap of 50% (more windows might be used to filter noise). The choice of only two windows transforms the  $\sigma(\bar{I}[k])$  operator into a  $\Delta(I[k])$  operator.  $\Delta(I[k])$  is evaluated per “bin”  $[k]$ . Since any variation can be seen as “non steady-state”, it is sufficient to map the data vector to a single value by a maximum norm. (Euclidean norm might work as well, with smoother output). The criterion can be made less prone to noise if the variances  $[k]$  are normalized by the expectation value of the main amplitude, rather than the expectation value  $[k]$ . This results in

$$y_{randomness} = \max \left( \frac{|A[k[t_x]]|^2 - |A[k[t_x + \Delta T]]|^2}{|A[k_{base}(t_x)]|^2} \right) \forall k \quad (34)$$

The SSI delay needs to be kept to a minimum, where delay is proportional to the window length, which in turn is proportional to the resolution of the DFT spectrum. The minimum delay is attained, when each band restricted variation is included by one bin each, but the window is not “flat top” whilst the resolution is high enough to prevent overlap with the adjacent harmonic by the window. Since we assume that all non-steady-state-caused distortion is centered around the base-frequency and the harmonics, the set of all  $k$  in criterion (34) can be limited to all bins which represent a harmonic of  $f_{base}$ . With the usual notation of expressing the number of the bins by their equivalent frequency, the  $k$ s in (34) are replaced by  $k = h \cdot f_{base}$ , with  $h = [1..M]$ . Inserting an additional  $\epsilon$  in the denominator to prevent division by zero and influence of noise directly results in

$$y_{THD-similar} = \max \left( \frac{|A[h \cdot f_{base}[t_x]]|^2 - |A[h \cdot f_{base}[t_x + \Delta T]]|^2}{|A[f_{base}(t_x)]|^2 + \epsilon \cdot |A_{nom}|^2} \right) \quad (35)$$

$\forall h \in [1..M]$

The windows of type Bartlett, Hamming or Hanning are especially recommended due to their small 3dB peak width of 1.2736,1.3008 and 1.4382 bins. For these windows the resolution of the spectrum should be at least  $1/3 \cdot f_{base}$  to prevent overlap.

## References

- Bünthe, T. Recording of Model Frequency Responses and Describing Functions in Modelica, *Proceedings of the 8th International Modelica Conference*, 2011.
- Brown, P. R. and Rhinehart, R. R.. Demonstration of a method for automated steady-state identification in multivariable systems. *Hydrocarbon processing* 79:79-83, 2000.
- Cao, S. and Rhinehart, R. R.. An efficient method for on-line identification of steady state, 5:363 - 374, 1995.
- Cooley, J. W. and Tukey, J. W.. An algorithm for the machine calculation of complex Fourier series. *Math. Comput.* 19:297-301, 1965.
- Debnath, L. and Shah, F. A.. *Wavelet transforms and their applications*. : Springer, 2002.
- Demiray, T.. *Simulation of Power System Dynamics using Dynamic Phasor Models*. Ph.D. thesis, ETH Zurich, 2008.
- Gao, J., Ji, Y., Bals, J. and Kennel, R.. Wavelet library for Modelica, *Proceedings of the 10th International Modelica Conference; March 10-12; 2014; Lund; Sweden*, 2014.
- Heinzel, G., Rüdiger, A., and Schilling, R.. *Spectrum and spectral density estimation by the Discrete Fourier transform (DFT), including a comprehensive list of window functions and some new at-top windows...*, online. [http://www.rssd.esa.int/SP/LISAPATHFINDER/docs/Data\\_Analysis/GH\\_FFT.pdf](http://www.rssd.esa.int/SP/LISAPATHFINDER/docs/Data_Analysis/GH_FFT.pdf), 2002.
- IEEE. Recommended Practice and Requirements for Harmonic Control in Electric Power Systems. *IEEE Std 519-2014 (Revision of IEEE Std 519-1992)* :1-29, 2014.
- Isermann, R.. *Fault-diagnosis systems: an introduction from fault detection to fault tolerance*. Springer (Ed.). : Springer Science & Business Media, 2006.
- Jiang, T., Chen, B. and He, X.. Industrial application of Wavelet Transform to the on-line prediction of side draw qualities of crude unit. *Computers & Chemical Engineering* 24:507-512, 2000.
- Jiang, T., Chen, B., He, X. and Stuart, P.. Application of steady-state detection method based on wavelet transform. *Computers & Chemical Engineering* 27:569 - 578, 2003b.
- Kelly, J. D. and Hedengren, J. D.. A steady-state detection (SSD) algorithm to detect non-stationary drifts in processes. *Journal of Process Control* 23:326-331, 2013.
- Korbel, M., Bellec, S., Jiang, T. and Stuart, P.. Steady state identification for on-line data reconciliation based on wavelet transform and filtering. *Computers & Chemical Engineering* 63:206-218, 2014.
- Krause, P. C., Wasynczuk, O. and Sudhoff, S. D.. *Analysis of Electric Machinery and Drive Systems*. : WileyBlackwell, 2002.
- Kuhn, M. R., Otter, M. and Giese, T.. Model Based Specifications in Aircraft Systems Design, *11th international Modelica Conference*, 2015.
- Kuhn, M. R., Rekik, M. and Bals, J.. Modelling and Use of an Aircraft Electrical Network Simulation for Harmonics Consideration in Generator Design, *SAE Technical Paper*, 2012.
- Mallat, S.. *A wavelet tour of signal processing: the sparse way*. : Academic press, 2008.
- Marple, S. L. and Marino, C.. Coherence in signal processing: a fundamental redefinition, *Signals, Systems and Computers, 2004. Conference Record of the Thirty-Eighth Asilomar Conference on* 1:1035-1038 Vol.1, 2004.
- US Department of Defense. *Aircraft electric power characteristic*. <http://www.wbdg.org/ccb/FEDMIL/std704f.pdf>, 2004.
- Oppenheim, A. V.. *Discrete-time signal processing*. : Pearson Education India, 1999.
- Oppenheim, A. V. and Schaffer, R. W.. *Zeitdiskrete Signalverarbeitung*. : Oldenbourg Wissenschaftsverlag, 1998.
- Pollok, A. and Bender, D.. Using Multi-objective Optimization to Balance System-level Model Complexity, *Proceedings of the 6th International Workshop on Equation-Based Object-Oriented Modeling Languages and Tools* :69-78, 2014.
- Saber. *Integrated Environment for Physical Modeling and Simulation*. Synopsys, I., [www.synopsys.com/prototyping/saber](http://www.synopsys.com/prototyping/saber), 2016.
- Schupp, G.. *Numerische Verzweigungsanalyse mit Anwendungen auf Rad-Schiene-Systeme*. Ph.D. thesis, Universität Stuttgart, 2003.
- Welch, P.. The use of fast Fourier transform for the estimation of power spectra: A method based on time averaging over short, modified periodograms. *IEEE Transactions on Audio and Electroacoustics* 15:70-73, 1967.